Changes in the African monsoon region at medium-term time horizon using 12 AR4 coupled models under the A1b emissions scenario

Article

Published Version

Open Access

It is advisable to refer to the publisher's version if you intend to cite from the work. See Guidance on citing.

RMetS

Royal Meteorological Society

Changes in the African monsoon region at medium-term time horizon using 12 AR4 coupled models under the A1b emissions scenario

Bernard Fontaine,* Pascal Roucou and Paul-Arthur Monerie
Centre de Recherches de Climatologie, UMR5210, CNRS/University of Burgundy, Dijon, France

*Correspondence to:
Bernard Fontaine, Centre de Recherches de Climatologie, UMR5210, CNRS/University of Burgundy, Dijon, France.
E-mail: fontaine@u-bourgogne.fr

Abstract

This study documents simulated precipitation and circulation changes through the 20C3M and A1b scenarios. It portrays a robust pattern, associating rainfall deficits in subtropical regions with rainfall excesses over West Africa, except in Northern Senegal and Mauritania, with a significant enhancement of both the April–June rainy season in 10/12 models and of the July–September rainy season in 8/12 models. Eastward to 5 °W a northward shift in the latitude of the moisture flux convergence at 850 hPa is evident in 10/11 models (+0.58° in mean) and a southward shift in 6/11 models in the western region (−0.24°) is observed. Copyright © 2011 Royal Meteorological Society

Keywords: African monsoon; climate change; precipitation; West Africa

1. Introduction

Some authors asserted that the partial recovery of Sahel precipitation since the 1990s could be a response to greenhouse gas forcing through an increased temperature contrast between land and ocean, since a wetter Sahel might follow from an enhanced warming of land compared to oceans, which would be responsible for driving a stronger monsoonal flow inland (Paeth and Hense, 2004). For Hoerling *et al.* (2006), Maynard *et al.* (2002) and Haarsma *et al.* (2005) a future wetter Sahel can be conceived as the response to a reversal in sea surface temperature pattern in the Atlantic Ocean due either to a reduction of aerosol loading or to the Atlantic multi-decadal oscillation. However, it could be premature to take this partial rainfall amelioration as evidence of a global warming signature, given the likely influence of internal variability on the inter-hemispheric sea surface temperature (SST) gradients that influence Sahel rainfall, as well as the influence of aerosol variations (Christensen *et al.*, 2007) and the flawed representations of the West African monsoon (WAM) climate (Cook and Vizy, 2006). However, recently, Giannini (2010) has pointed out that the increase in anthropogenic greenhouse gases drives a direct continental change in the Sahel region: the increase in net terrestrial radiation at the surface is amplified by the water vapour feedback which increases evaporation, favouring vertical instability and near-surface convergence.

Some AR4 20C3M simulations (20th century runs using historical GHG concentrations, 1871–2000), can produce unrealistic variability in the Sahel with systematic errors and large model differences (Christensen *et al.*, 2007; Paeth *et al.*, 2009). This is partly due to the different parameterisations of clouds and convection, to the omission of dynamic vegetation (Giannini *et al.*, 2003) and to the quasi-absence of feedbacks from dust aerosol production and from future land surface modification in projections.

The goal of this paper is to identify precipitation changes and associated atmospheric signals in North Africa at medium-term time horizon through a multi-model (MM) ensemble approach based on the 20C3M simulations and A1b emissions scenario from 12 ocean–atmosphere coupled models. We will focus on the April–June (AMJ) and July–September (JAS) rainy seasons observed in the Guinean and Sudan-Sahel, respectively. These choices are hence different from most studies conducted to date including the last IPCC report which concentrated more on the June–August climate changes between years 1980–1999 and 2080–2099, and concluded on non-robust response with modest moistening in the Sahel with little change on the Guinean coast (Christensen *et al.*, 2007). The choice of a relatively short time horizon (50 years) may also increase the generality of the results since before 2050, CO_2 emissions and concentrations in A1b are very similar to those projected by scenarios from the A2 family.

2. Data and methods

The A1b scenario provides a good mid-line scenario for CO_2 emission and economic growth and supposes a balanced emphasis on all energy sources. The MM approach is based on 12 runs issued from 12 different coupled models (Table I more details on http://www.ipcc.ch): Joly and Voldoire (2009) have shown that this set offers a representative sample of the

Table I. The 12 models and groups. More details in Randall *et al.* (2007), their Table 8.1 (pp. 597–598).

Models	Grids longitude x latitude x level	Models	Grids longitude x latitude x level
CCMA: Canadian Centre for Climate Modelling and Analysis, Canada	96 × 48 × 17	MIROC : Center for Climate System Research, + Institute for Environmental Studies, + Frontier Research Center for Global Change, Japan	128 × 64 × 17
GFDL: Geophysical Fluid Dynamics Laboratory, USA	144 × 90 × 17	NCAR : National Center for Atmospheric Research, USA	256 × 128 × 17
IPSL: Institut Pierre Simon Laplace, France	96 × 72 × 17	CSIRO: CSIRO Atmospheric Research, Melbourne, Australia	192 × 96 × 17
MRI: Meteorological Research Institute, Japan	128 × 64 × 17	INMCM: Institute for Numerical Mathematics, Russia	72 × 45 × 17
CNRM: Centre National de Recherches Meteorologiques, France	128 × 64 × 17	MPI: Max Planck Institute for Meteorology, Germany	192 × 96 × 16
GISS: Goddard Institute for Space Studies, New York, NY, USA	72 × 45 × 17	UKMO: Met Office, UK	96 × 73 × 15

performance of state-of-the art coupled models without any type of a priori consideration.

Precipitation change and associated signals are estimated by comparing the seasonal rainfall outputs simulated by the 12 models, between the years 1960 and 1999, the 'current period', and 2031–2070, the 'near future', using in cooperation (1) the MM approach, (2) the 'one model one vote' concept (Santer *et al.*, 2009) and (3) individual differences taken with respect to each model climatology. The 'current period' includes a comprehensive set of both abnormally wet years (in the 1960s and 1990s) and abnormally dry years (within the 1970s and 1980s).

The CRU TS 2.1 at 0.5° resolution (Mitchell *et al.*, 2002) and the GPCP at 2.5° (Adler *et al.*, 2003) datasets will be used as observational reference for estimating the continental rainfall.

The simulated changes will be presented as seasonal means and composite fields and through (1) rainfall indexes depicting the AMJ Guinean rainy season and the JAS monsoon season, (2) atmospheric indexes describing the mean location of moisture flux convergence at 850 hPa, and (3) near-surface temperatures, moisture fluxes and meridional gradients of moist static energy over West Africa.

3. Rainfall patterns

The JAS ensemble mean (Figure 1(a)) shows first that models have difficulties in reproducing the observed northward penetration of the rain belt deep into the continent: this belt stands abnormally southward (7–8°N vs ~10°N in observation) due to an insufficient simulated upwelling off the West Coast by 3°C off the southwest coast (Christensen *et al.*, 2007).

Nonetheless, the precipitation change (Figure 1(b)) shows that the largest drying is simulated within the whole Mediterranean and Southern European domain in agreement with conclusions for the end of the 21st century (Christensen *et al.*, 2007). However, our
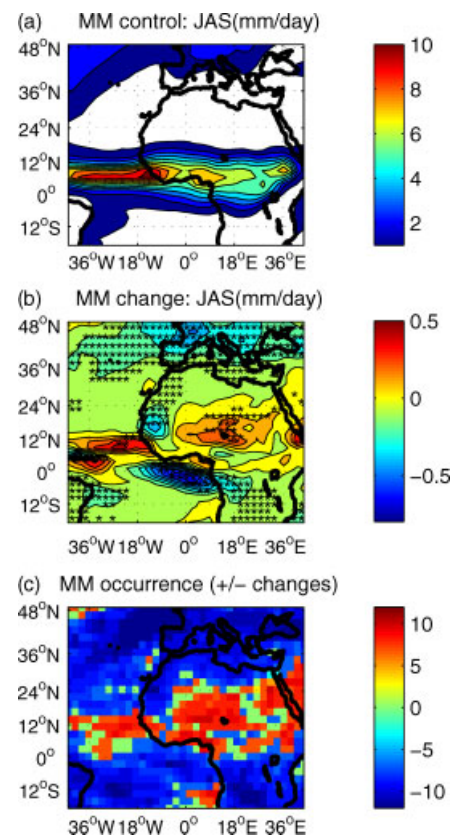
Figure 1. Simulated rainfall in JAS as simulated by the 12 models listed in Table I. (a) Mean rainfall for the current period in mm/day; (b) precipitation change in mm/day between years 2031–2070 and 1960–1999; the superimposed asterisks refer to significant differences at $p = 0.05$ using a Student t-test; (c) number of models simulating a deficit (negative values) or an excess (positive values) by grid-points, i.e. the scores range either between +7 and +12 or between −7 and −12: +7 (−7) means that 7 models out of 12 simulate increasing (decreasing) rainfall and +12 (−12) that all models produce an excess (a deficit).

results exhibit a significant composite pattern with increasing rainfall over the central and eastern Sahel regions and negative differences in the Guinean Gulf and western Sahel: rainfall excesses are encountered

Table II. July–September (JAS) rainfall means (in mm/day), interannual standard deviations (STD) and coefficients of variation (STD/mean) in observations (CRU, underlined) and individual simulations (period 1960–1999) averaged over the western (20 W–0°) and eastern (0°–30 °E) parts of West Africa (5°N–20°N): WAMW and WAME, respectively.

WAMW	CRU	GPCP	GFDL	MIROC	UKMO	CCCMA	NCAR	MPI	GISS	CSIRO	INMCM	CNRM	MRI	IPSL
Mean	**5.6**	**5.9**	8.6	7.1	**5.8***	**5.6***	**5.4***	**5.4***	4.5	4.3	3.7	3.3	3.2	3.2
STD	**0.7**	**0.7**	0.8	0.7	0.6	0.5	0.3	0.5	0.7	0.4	0.4	0.5	0.4	0.3
CV %	**12.7**	**11.7**	9.2	9.8	10.0	8.4	5.3	9.5	14.9	8.6	11.5	13.8	10.8	8.5

WAME	CRU	GPCP	CNRM	MIROC	GFDL	CCCMA	NCAR	UKMO	CSIRO	MPI	MRI	GISS	INMCM	IPSL
Mean	**4.3**	**4.3**	5.6	5.6	4.8	**4.5***	**4.4***	**4.2***	3.7	3.4	3.2	2.7	2.5	1.9
STD	**0.5**	**0.5**	0.5	0.6	0.7	0.4	0.2	0.5	0.3	0.3	0.2	0.4	0.3	0.1
CV %	**11.4**	**11.1**	9.6	11.5	13.8	8.2	4.6	12.5	8.4	10.3	6.2	13.8	11.6	7.2

Model acronyms are arranged from left to right in descending order relatively to the mean. The simulated JAS means not significantly different from observations regarding a Student t-test at $p = 0.05$ are bolded with an asterisk.

by 12°N in the eastern Atlantic and central Sahel in association with rainfall deficits over the Gulf of Guinea. This supposes a deeper northward penetration of the rain belt associated with an enhancement of the monsoon circulation since GES scenarios produce stronger warming in northern tropical Atlantic, southern Europe and Mediterranean areas than in the moister tropics (Christensen *et al.*, 2007). The generated SST anomaly pattern in the Atlantic and the Mediterranean is favourable to a more northward excursion of the monsoon (Garcia-Serrano *et al.*, 2008; Fontaine *et al.*, 2009) while the meridional surface temperature anomaly gradient over West Africa tends to shift farther north the African Easterly Jet which is also associated with a larger rainfall over Sahel (Hourdin *et al.*, 2010).

Figure 1(c) displays the number of models simulating positive and negative JAS differences after giving to each model the same weight (see the caption). Rainfall deficits are observed in subtropical regions and rainfall excesses over a large WAM area, except in Northern Senegal and Mauritania. The largest positive scores (+8) are encountered over central Sahel by 12°N, just northward to the mean location of the rain belt in the models (Figure 1(a)); the largest negative scores (< −10) are located in the northern subtropics and south of the equator. Precipitation change in West Africa is, overall, positive and denotes a deeper penetration of the monsoon into the continent mainly eastward to 10 °E. Conversely, the change is negative over areas of large-scale subtropical subsidence, especially in the Mediterranean and Eastern Atlantic regions. Interestingly precipitation changes simulated by the 12 individual models (not shown) indicate that most models simulate similar patterns to those displayed in Figure 1(b)–(d), in particular CNRM, NCAR, CCCMA, UKMO and MPI.

3.1. Regional rainfall and associated changes

Regional indexes have been first defined by averaging in each model the seasonal rainfall amounts on two specific key-regions: the AMJ season in the Gulf of Guinea (Eq–5N; 20 W–10E) and the JAS season over the western and eastern continental parts of West Africa (Table II). Most models are often close to the observed mean, except those listed at right, but tend to underestimate the inter-annual standard deviations and coefficients of variation because the inter-annual variability of SST is very weak in the Gulf of Guinea (Joly and Voldoire, 2010).

Mean annual evolutions (Figure 2(a)–(c)) show that (1) only one half of the models reproduce a clear seasonal cycle while the mean model ensemble fails on this aspect and (2) the models which perform at best on a region or season are not necessarily successful on other regions and seasons, except for INMCM (Institute for Numerical Mathematics), IPSL (Institut Pierre Simon Laplace) and MRI (Meteorological Research Institute) which simulate the lowest seasonal cycles and rainfall amounts.

Composites in Figure 2(d)–(i) display, for each model and month, the precipitation changes: a clear enhancement of AMJ amounts is found over the equatorial Atlantic, with ten boxes showing significant excesses in Figure 2(d) (*vs* two deficits). On the whole, 10 models out of 12 produce an AMJ increase of the median and quartile values (Figure 2(g)). Changes in JAS are less obvious on the western part of Africa: no signal with the multi-ensemble mean (Figure 2(h)) and only 6/3 models produce significant positive/negative differences (Figure 2(h)). By contrast, over the eastern part (Figure 2(i)), the MM ensemble and 9/12 models simulate higher rainfall.

Such modifications in Sahelian rainfall increase and shift in latitude are associated with coherent changes in the West African monsoon circulation. For example, the moisture flux convergence at 850 hPa in boreal summer is also shifted northward (southward) (Figure 2(j) and (k)): eastward (westward) to the zero longitude, this displacement is observed in 10/11 (6/11) individual models with a +0.58° (−0.24°) shift in the MM. These values are significant at $p = 0.05$.

Changes in surface air temperature and moisture flux at 925 hPa are also significant. Thus, Figure 3(b) and (d) denotes a reinforced monsoon flux over
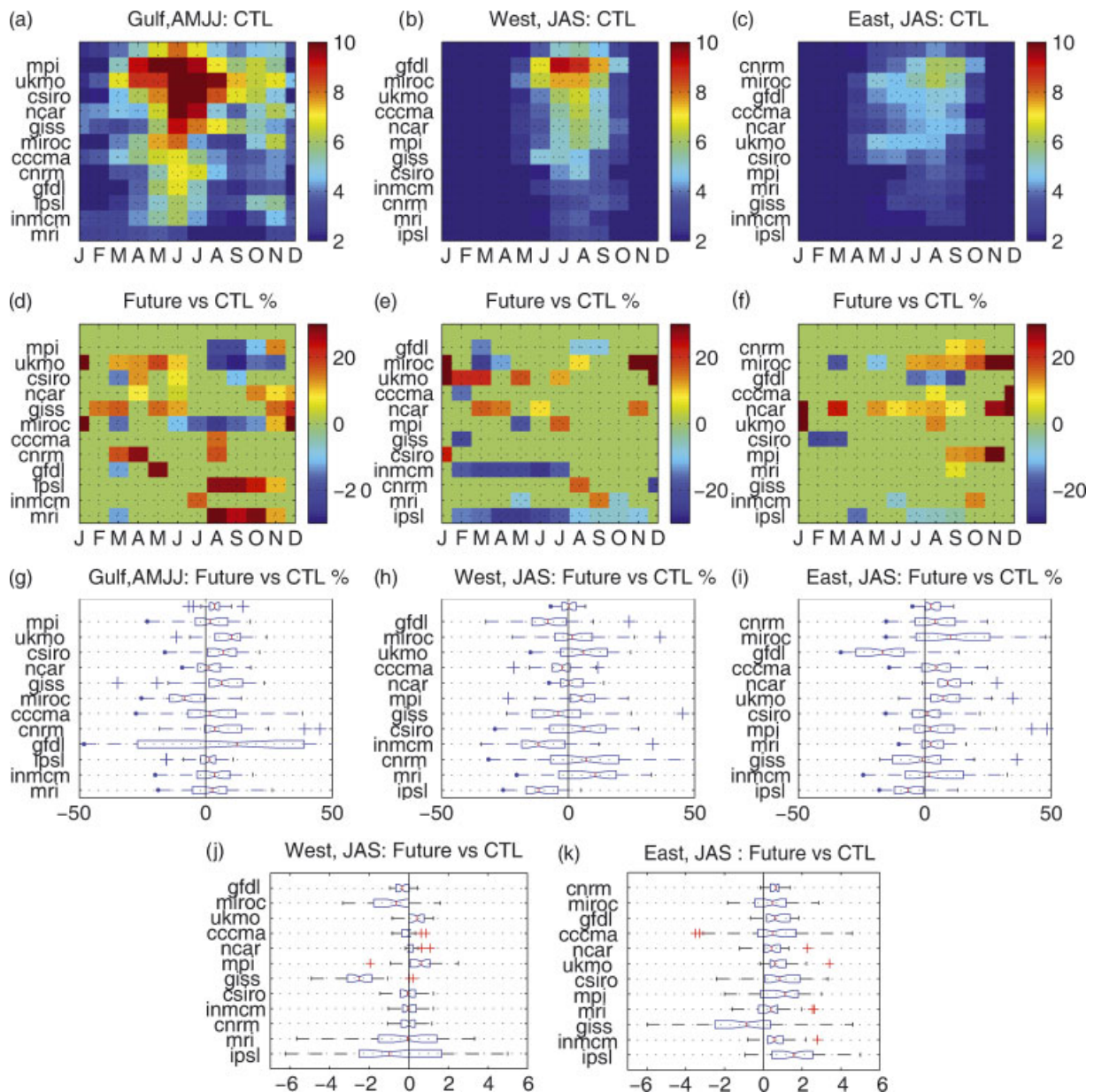
Figure 2. Simulated seasonal indexes averaged over key-regions. (a–c) Mean annual rainfall evolutions over the Gulf of Guinea (Eq–5N; 20 W–10E) from April to June (column 1) and over the western (5N–20N; 20 W–0E) and eastern (5N–20N; 0E–30E) continental parts of West Africa (columns 2 and 3). Model acronyms (*y*-axis) are sorted in descending order regarding individual seasonal amounts with the mean model ensemble at top; (d–f) significant ($p = 0.05$) precipitation change expressed in percents between years 1960–1999 and 2031–2070; (g–i) notched-box plot as robust estimate of the uncertainty about the medians for box to box comparison. Each box has lines at the lower quartile, median, and upper quartile values, all expressed in percentages of precipitation change. Lines extending from each end of the box show the extent of the rest of the data between −50% and +50%; and (j and k) as (g–i) but for the latitudinal location in degree of the centroid of the moisture flux convergence at 850 hPa averaged over a western (15 °W–5 °W; 0°N–14°N) and a central-eastern (5 °W–20 °E; 0°N–20°N) African regions. Here, only 11 models out of 12 are considered since no moisture data were available in UKMO (Met Office, UK).

West Africa and India, in association with continental warming over the northern tropical deserts and, in JAS, all around the Mediterranean. This thermal pattern tends to strengthen both the Saharan heat low (Figure 3(b) and (d)) and the meridional temperature gradients known to be linked to the horizontal moist static energy gradients driving the monsoon circulation (Fontaine *et al.*, 1999). It is worth noting that all individual models and the MM mean produce such a temperature gradient enhancement during the two AMJ and JAS rainy seasons over the Guinean

and Sahelian regions (Figure 3(e) and (f)). Since the moisture and thermal gradients impact the AEJ location in regional climate model outputs (Bamba Sylla *et al.*, 2009), these changes could therefore impact the future African monsoon.

5. Conclusion

The goal of this study was to document the AMJ and JAS precipitation changes in the African monsoon
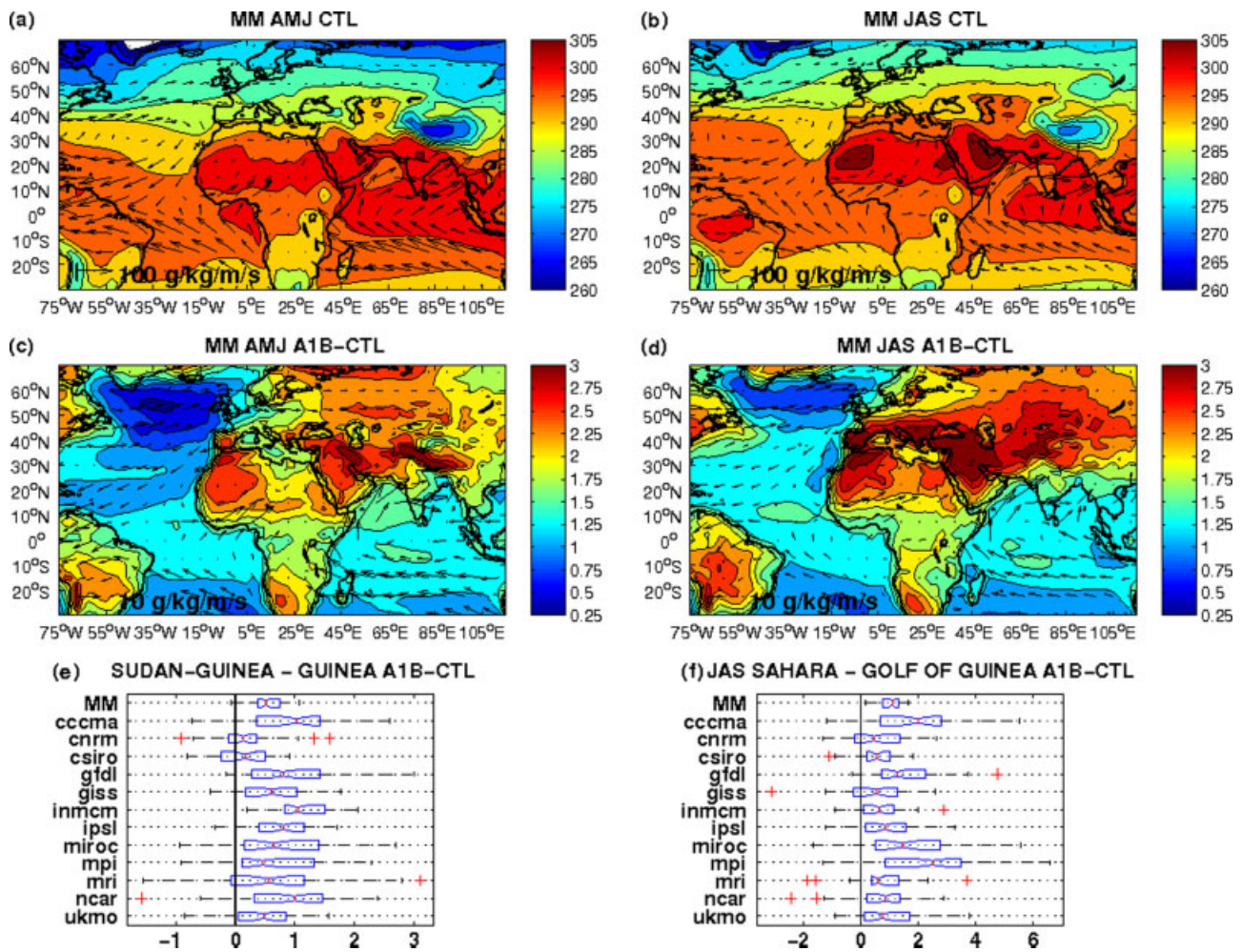
Figure 3. Simulated changes in air temperature near the surface, in moisture flux at 925 hPa (maps), and in air temperature gradients (boxplots) in April–June (AMJ) (left) and July–September (JAS) (right); (a and b) Temperature in tenth of °C and moisture fluxes in g/kg/m/s from the ensemble mean (1960–1999); (c and d) differences in air temperature at 2 m and in moisture fluxes at 925 hPa between years 1960–1999 and 2031–2070; (e and f) notched-box plot (as in Figure 2(g)–(i)), but for changes (in °C) in meridional air temperature gradient at 2 m between 10 °W and 0° longitude. In AMJ, the gradient refers to the difference between values averaged over (7.5 °N–12.5 °N) and over (5 °S–Eq) while in JAS the gradient is the difference between (20°N–15°N) and (5 °S–Eq).

region by contrasting the 40-year periods 1960–1999 and 2031–2070. The results showed that model accuracy depends on the ability to reproduce the observed mean seasonal cycle. The simulated changes around the middle of this century are spatially coherent and locally significant. They reproduce a typical anomaly pattern contrasting rainfall deficits in the subtropical regions, and rainfall excesses over a large West African monsoon area, except in Northern Senegal and Mauritania.

Analyses of a few key-regional indices also denoted lower (higher) occurrence of anomalous dry (wet) rainy seasons. Rainfall increases are attested in 10 models out of 12 during the April–June rainy season in the Gulf of Guinea, and in 8 models out of 12 for the JAS amounts over the central and eastern Sahel. In JAS the rainfall pattern contrasts excesses around 12°N in the eastern Atlantic and central Sahel and deficits over the Gulf of Guinea. Moreover, eastward to the zero longitude a northward shift in latitude of the moisture flux convergence

at 850 hPa is evident in 10/11 models (+0.58° in mean) but a southward shift in 6/11 models in the western region (−0.24°) is observed. Associated changes in near-surface temperature, moisture fluxes and meridional temperature gradients are significant in near-all models and denote a more vigorous monsoon penetrating deeper into the West African continent. In a future paper we will focus on the atmospheric conditions associated with the global warming to explain the differential effect on the western and central-eastern Sahel, and therefore contribute to reduce uncertainty on the global warming effect in the region.

Acknowledgements

References

Adler RF, Huffman GJ, Chang A, Ferraro R, Xie P, Janowiak J, Rudolf B, Schneider U, Curtis S, Bolvin D, Gruber A, Susskind J, Arkin P, Nelkin E. 2003. The version-2 global precipitation climatology project (GPCP) monthly precipitation analysis (1979-present). *Journal of Hydrometeorology* **4**: 1147–1167.

Bamba Sylla M, Coppola E, Mariotti L, Giorgi F, Ruti PM, Dell'Aquila A, Bi X. 2009. Multiyear simulation of the African climate using a regional climate model (RegCM3) with the high resolution ERA-interim reanalysis. *Climate Dynamics* Online publication date: 2 July 2009.

Christensen JH, Hewitson B, Busuioc A, Chen A, Gao X, Held I, Jones R, Kolli RK, Kwon WT, Laprise R, Magaña Rueda V, Mearns L, Menéndez CG, Räisänen J, Rinke A, Sarr A, Whetton P. 2007. Regional climate projections. In *Climate Change 2007: The Physical Science Basis*. Cambridge University, Press: Cambridge.

Cook KH, Vizy EK. 2006. Coupled model simulations of the West African monsoon system: 20th century simulations and 21st century predictions. *Journal of Climate* **19**: 3681–3703.

Fontaine B, Garcia-Serrano J, Roucou P, Rodriguez-Fonseca B, Losada T, Chauvin F, Gervois S, Sivarajan S, Ruti P, Janicot S. 2009. Impacts of warm and cold situations in the Mediterranean Basins on the West African monsoon: observed connection patterns (1979–2006) and climate simulations. *Climate Dynamics* ISSN0930-7575 (Print) 1432-0894 (Online), DOI 10.1007/s00382-009-0599-3.

Fontaine B, Philippon N, Camberlin P. 1999. An improvement of June–September rainfall forecasting in the Sahel based upon region April–May moist static energy content (1968–1997). *Geophysical Research Letter* **26**: 2041–2044.

Garcia-Serrano J, Losada T, Rodriguez-Fonseca B, Polo I. 2008. Tropical Atlantic variability modes (1979–2002). Part II: time-evolving atmospheric circulation related to SST-forced tropical convection. *Journal of Climate* **21**(24): 6476–6497.

Giannini A. 2010. Mechanisms of climate change in the semi-arid African Sahel. the local view. *Journal of Climate* **23**: 743–756.

Giannini A, Saravanan R, Chang P. 2003. Oceanic forcing of Sahel rainfall on interannual to interdecadal time scales. *Science* **302**: 1027–1030.

Haarsma RJ, Selten F, Weber N, Kliphuis M. 2005. Sahel rainfall variability and response to greenhouse warming. *Geophysical Research Letters* DOI 10.1029/2005GL023232.

Hoerling MP, Hurrell JW, Eischeid J. 2006. Detection and attribution of 20th century Northern and Southern African monsoon change. *Journal of Climate* **19**(16): 3989–4008.

Hourdin F, Musat I, Guichard F, Ruti PM, Favot F, Filiberti MA, Pham M, Grandpeix JY, Polcher J, Marquet P, Boone A, Lafore JP, Redelsperger JL, Dell'aquila A, Losada Doval T, Khadre Traore A, Gallée H. 2010. AMMA-model intercomparison project. *Bull. Amer. Meteor. Soc.* **91**: 95–104.

Joly M, Voldoire A. 2009. Influence of ENSO on the West African monsoon: temporal aspects and atmospheric processes. *Journal of Climate* **22**(12): 3193–3210.

Joly M, Voldoire A. 2010. Role of the Gulf of Guinea in the inter-annual variability of the West African monsoon: what do we learn from CMIP3 coupled simulations? *International Journal of Climatology* **30**: 1843–1856 DOI 0.1002/joc.2026.

Maynard K, Royer JF, Chauvin F. 2002. Impact of greenhouse warming on the West African summer monsoon. *Climate. Dynamics* **19**: 499–514.

Mitchell TD, Hulme M, New M. 2002. Climate data for political areas. *Area* **34**: 109–112.

Paeth H, Hense A. 2004. SST versus climate change signals in West African rainfall: 20th-century variations and future projections. *Climatic Change* **65**(1–2): 179–208.

Paeth H, Born K, Girmes R, Podzun R, Jacob D. 2009. Regional climate change in tropical and northern Africa due to greenhouse forcing and land use changes. *Journal of Climate* **22**: 114–132.

Randall DA, Wood RA, Bony S, Colman R, Fichefet T, Fyfe J, Kattsov V, Pitman A, Shukla J, Srinivasan J, Stouffer RJ, Sumi A, Taylor KE. 2007. Cilmate Models and Their Evaluation. *Climate Change 2007: The Physical Science Basis*. Contribution of Working Group I to the Fourth Assessment Report of the Intergovernmental Panel on Climate Change [Solomon S, Qin D, Manning M, Chen Z, Marquis M, Averyt KB, Tignor M and Miller HL (eds.)]. Cambridge University Press: Cambridge, United Kingdom and New York, NY, USA.

Santer BD, Taylor KE, Gleckler PJ, Bonfils C, Barnett TP, Pierce DW, Wigley TML, Mears C, Wentz FJ, Braggemann W, Gillett NP, Klein SA, Solomon S, Stott PA, Wehner MF. 2009. Incorporating model quality information in climate change detection and attribution studies. *Proceedings of the National Academy of Sciences* **106**(35): 14778–14783.